



## A SEARCH FOR DEBRIS DISKS AROUND NEARBY LATE-M DWARFS

*Nguyen Thanh Dat<sup>1,2\*</sup>, Phan Bao Ngoc<sup>1</sup>*

<sup>1</sup> Department of Physics, VNUHCM - International University

<sup>2</sup> Faculty of Physics and Engineering Physics, VNUHCM - University of Science

Received: 02/7/2018; Revised: 20/8/2018; Accepted: 21/9/2018

### ABSTRACT

*In this paper, we present our search for debris disks in a sample of nearby late-M dwarfs based on infrared data of the Wide Infrared Survey Explorer. Using archival data, we constructed spectral energy distributions of these targets to detect their infrared excess. We detected infrared excess only in one target. This late-M dwarf is an excellent benchmark for further study of disks around very low-mass objects.*

**Keywords:** brown dwarfs, debris disks, infrared excess, planet formation, very low-mass stars.

### TÓM TẮT

*Tìm kiếm đĩa tàn dư xung quanh các sao lùn kiểu phổ M-trễ  
nằm trong vùng lân cận Mặt Trời*

*Trong bài báo này, chúng tôi tìm kiếm đĩa tàn dư ở một mẫu gồm các sao lùn có kiểu phổ M-trễ nằm trong vùng lân cận Mặt Trời bằng dữ liệu vùng hồng ngoại từ kính viễn vọng không gian hồng ngoại WISE. Sử dụng các dữ liệu có sẵn, chúng tôi xây dựng phổ phân bố năng lượng của các vật thể trong mẫu để phát hiện các ứng cử viên có bức xạ hồng ngoại dư. Chúng tôi phát hiện bức xạ hồng ngoại dư ở duy nhất tại một sao lùn M. Đây sẽ là mẫu sao lùn tiêu biểu cho các nghiên cứu tiếp theo về đĩa xung quanh các sao có khối lượng rất thấp.*

**Từ khóa:** sao lùn nâu, đĩa tàn dư, bức xạ hồng ngoại dư, sự hình thành hành tinh, sao có khối lượng rất thấp.

### 1. Introduction

Most stars are born with primordial gas and dust disks (i.e., protoplanetary disks) where the process of planet formation occurs. The primordial disks around stars have almost disappeared in 6 Myr [1]. Subsequently, the disks left over the process of planet formation are so-called debris disks, which are made of planetesimals (e.g., asteroids and comets). In these disks, dust is continuously generated by collisions and evaporation of planetesimals. The study of circumstellar disks (i.e., primordial and debris disks) has significantly improved our understanding of stellar and planetary evolution [1], [2].

Theoretical models have shown that planets can also form in the disks of young brown dwarfs (BDs, 13-75  $M_{\text{Jupiter}}$ ) and very low-mass (VLM,  $< 0.35 M_{\text{Sun}}$ ) stars [3]. The

\* Email: ngthanhdatt0491@gmail.com

models suggest that BDs and VLM stars can harbor more rocky planets than giant planets. Recent discoveries of planetary systems around VLM stars, such as Kepler-42 (M5,  $\sim 0.13 M_{\text{Sun}}$ ) with three Earth-like planets [4] and TRAPPIST-1 (M8,  $\sim 0.08 M_{\text{Sun}}$ ) with seven Earth-like planets [5], [6], have strongly supported these models. Therefore, detecting and studying circumstellar disks around VLM objects are important in understanding how rocky planets form around these objects.

Debris disks have been found in many different types of stars, from early-type (e.g., A stars) and solar-type stars (e.g., FGK stars) to M dwarfs [7]-[9]. However, the number of debris disks detected around M dwarfs, particularly late-M (later than M5-M6) dwarfs and BDs, remains relatively small. Four early-M dwarfs with debris disks detected so far are: GJ 182 (M0.5), Au Mic (M1), GJ 842.2 (M0.5) and GJ 581 (M3) [10]-[12]. Recently, five circumstellar disks have also been detected around VLM stars and BDs [13], [14].

We could detect debris disks around stars through the excess in flux density at IR wavelengths that is the so-called IR excess. Dust in debris disks absorbs radiation from host stars and re-emits energy at IR wavelengths, resulting in an IR excess. The IR excess has been used as a tool to detect debris disks [7]-[9]. We have therefore carried out a search for infrared excess in a sample of 86 nearby late-M dwarfs. Using Deep Near Infrared Survey (DENIS), Two Micro All Sky Survey (2MASS) and the Wide Infrared Survey Explorer (WISE) photometry, we constructed spectral energy distributions (SEDs) of our targets in order to identify candidates that show IR excesses at WISE wavelengths. We then examined WISE images of these candidates to confirm their IR excess.

## 2. Sample

We selected 86 nearby late-M dwarfs with spectral types later than M5.0 (see Table 1). These late-M dwarfs have been identified by the DENIS survey (see [15], [16]-[20]). Their spectral types and distances have previously determined [15], [18]-[22], [23]. The 2MASS and WISE photometric data are available for all targets.

In Table 1, some of our targets also show the lithium absorption line at 6708 Å in their optical spectra as presented in our earlier works [20]: targets 11, 20, 26, 67 and 71. The presence of lithium in late-M dwarfs can be briefly interpreted as follows: According to theory of VLM objects [24], BDs with masses below  $60 M_{\text{Jupiter}}$  are not massive enough to burn lithium in their cores by the reaction  ${}^7\text{Li} + \text{p} \rightarrow 2 {}^4\text{He}$ . Thus, all BDs with masses in the range of 13 -  $60 M_{\text{Jupiter}}$  will preserve primordial lithium. Because BDs are fully convective, the lithium can be detected in their atmosphere. One should note that at young ages, some early-M dwarfs still have lithium because there is not enough time for completely depleting lithium in these stars. However, late-M dwarfs with temperature below 2790 K (M6 or later) that show the lithium absorption line at wavelength 6708 Å in their spectrum should be BDs [25].

Since all the targets in our sample have spectral types later than M5.0, and five of them (targets 11, 20, 26, 67 and 71) with detected lithium, they therefore have masses below the hydrogen-burning limit (i.e., BD masses) or very close to the substellar boundary (i.e., VLM stars).

*Table 1. Physical parameters of 86 nearby late-M dwarfs*

Target	Distance (parsecs)	SpT	References
(1)	(2)	(3)	(4)
1	21.0	M6.5	[19]
2	15.9	M5.5	[15]
3	26.3	M5.5	[15]
4	16.6	M6.0	[15]
5	26.8	M5.5	[15]
6	23.2	M6.0	[19]
7	17.0	M7.5	[19]
8	29.5	M6.0	[15]
9	24.3	M5.5	[19]
10	23.8	M8.0	[19]
11	23.3	M5.5	[19]
12	20.5	M7.5	[19]
13	27.1	M7.0	[19]
14	25.5	M5.5	[19]
15	17.2	M5.5	[19]
16	11.3	M8.5	[15]
17	25.7	M5.5	[19]
18	23.1	M5.5	[19]
19	19.7	M6.0	[19]
20	12.8	M7.0	[15]
21	18.1	M5.5	[18]
22	24.4	M6.0	[19]
23	24.7	M8.0	[15]
24	8.9	M7.5	[15]
25	12.1	M8.0	[19]
26	19.5	M6.5	[15]
27	23.4	M5.0	[19]
28	18.9	M5.0	[19]
29	9.1	M6.5	[20]
30	11.3	M6.0	[20]
31	27.9	M6.5	[22]
32	12.7	M6.5	[15]
33	21.1	M7.0	[23]

34	17.9	M7.0	[15]
35	20.8	M8.0	[19]
36	25.9	M6.0	[19]
37	4.5	M7.0	[15]
38	20.5	M6.0	[19]
39	25.7	M6.0	[19]
40	17.2	M8.0	[19]
41	23.4	M5.0	[19]
42	20.1	M5.0	[19]
43	9.7	M7.5	[15]
44	24.7	M5.5	[19]
45	29.2	M5.5	[19]
46	22.0	M6.0	[19]
47	19.4	M5.5	[19]
48	19.3	M6.0	[15]
49	14.6	M6.5	[15]
50	13.9	M6.0	[19]
51	24.7	M7.5	[19]
52	19.3	M5.0	[19]
53	10.1	M5.5	[20]
54	23.4	M5.0	[19]
55	10.0	M5.0	[20]
56	16.3	M7.5	[21]
57	22.8	M8.0	[19]
58	31.7	M5.0	[15]
59	26.7	M5.0	[19]
60	5.4	M8.0	[20]
61	10.5	M6.0	[15]
62	21.5	M5.0	[15]
63	17.7	M5.5	[15]
64	14.6	M6.0	[19]
65	24.9	M5.5	[19]
66	10.5	M6.0	[20]
67	10.4	M5.0	[20]
68	11.0	M6.0	[20]
69	22.1	M5.5	[15]
70	17.5	M6.0	[19]
71	22.9	M5.5	[15]
72	19.4	M6.0	[15]
73	27.0	M5.5	[15]

<b>74</b>	18.5	M5.5	[19]
<b>75</b>	14.1	M5.5	[15]
<b>76</b>	18.7	M5.0	[19]
<b>77</b>	25.8	M6.5	[15]
<b>78</b>	18.2	M5.5	[19]
<b>79</b>	18.2	M8.0	[15]
<b>80</b>	16.1	M5.0	[15]
<b>81</b>	16.5	M8.5	[15]
<b>82</b>	12.5	M5.5	[20]
<b>83</b>	11.6	M8.5	[15]
<b>84</b>	24.1	M5.0	[15]
<b>85</b>	19.2	M5.5	[15]
<b>86</b>	19.1	M8.5	[19]

*Column 1:* Target identification.

*Column 2:* Spectroscopic distances.

*Column 3:* Spectral types.

*Column 4:* References for distances and spectral types.

### 3. Method

#### 3.1. Spectral Energy Distributions of Targets

In order to detect IR excess, we constructed SEDs of all targets over a wide range of wavelengths, from optical, near-IR, and IR to mid-IR. We used DENIS (I-band: 0.79  $\mu\text{m}$ ) for optical, 2MASS for near-IR (J-band: 1.25  $\mu\text{m}$ , H-band: 1.65  $\mu\text{m}$ , and  $K_s$ -band: 2.17  $\mu\text{m}$ ) and WISE for IR and mid-IR (bands W1: 3.4  $\mu\text{m}$ , W2: 4.6  $\mu\text{m}$ , W3: 12  $\mu\text{m}$ , and W4: 22  $\mu\text{m}$ ). The magnitudes in these bands were converted to flux densities using the relationships given in [26], [27], and [28].

We then fitted these photometric data with NextGen model atmospheres of VLM stars and BDs [29] with effective temperature  $T_{\text{eff}}$  below 4000 K, surface gravity  $\log(g)$  ranging from 3.5 to 5.5, and metallicity  $[M/H] = 0.0$ . To find the best fitting of these models, we computed their averaged deviation using the following equation:

$$\sigma^2 = \frac{1}{N} \sum_{i=1}^N (F_{\lambda}^i - F_{\lambda,\text{mod}}^i)^2$$

where  $N$  is the number of photometric bands,  $F_{\lambda}^i$  is the observed flux at wavelength  $\lambda$  of each band,  $F_{\lambda,\text{mod}}^i$  is the theoretical flux at wavelength  $\lambda$  of each band. The best fit from the models that minimizes the averaged deviation is selected.

### 3.2. *Detection of infrared excess*

Based on the constructed SED of each object, we then searched for IR excesses at the WISE bands. We first compared the observed flux with the theoretical flux from the best-fit model in the WISE bands. Candidates with IR excess are identified if their observed flux is significantly larger than their theoretical flux at least in one band.

We then further examined WISE images of all candidates to confirm their real IR excess. We used DS9 (SAOImage, <http://ds9.si.edu>) to examine the WISE images in order to discard false-positive IR-excess candidates [9], [13]. A clear detection of IR excess should show a distinct source from the background.

## 4. Results and discussion

### 4.1. *Candidates with infrared excess*

Using the steps as described above, we detected 7 candidates that show IR excess: targets 29, 32, 34, 41, 42, 49 and 58. However, the IR excesses at 22  $\mu\text{m}$  in targets 29, 32, 34, 41, 42 and 49 are marginal (see Fig. 1) because the detection levels of IR excess in these six sources are below  $3\sigma$  ( $1\sigma$  is the error bar). Only target 58 shows strong IR excess at 4.6  $\mu\text{m}$  (a detection level of  $\sim 15\sigma$ ), 12  $\mu\text{m}$  ( $\sim 27\sigma$ ) and 22  $\mu\text{m}$  ( $\sim 9\sigma$ ).

Our further examination with WISE images shows that the IR excesses at 22  $\mu\text{m}$  in the six candidates (targets 29, 32, 34, 41, 42 and 49) are false-detections (see Sec. 3.2). We therefore conclude that there is no IR excess in these targets with the current data. For the case of target 58, the images in three bands W2, W3 and W4 show a clear detection of the source in all the three bands. Therefore, we confirm its IR excess.

### 4.2. *A new circumstellar disk around an M dwarf*

From our sample of 86 nearby late-M dwarfs, we have identified a unique candidate that shows strong IR excesses at 4.6  $\mu\text{m}$ , 12  $\mu\text{m}$  and 22  $\mu\text{m}$ . The IR excess can stem from dust in a primordial disk or a debris disk that surrounds the star. While protoplanetary disks mostly emit their excesses from the IR and onward, the excesses of debris disks are mainly in the mid-IR and beyond [5]. Since target 58 exhibits the excesses at both IR (4.6  $\mu\text{m}$ ) and mid-IR (12  $\mu\text{m}$  and 22  $\mu\text{m}$ ) wavelengths, its disk therefore could be either a protoplanetary disk or a debris disk.

## 5. Summary

In this paper, we present our preliminary result of a search for IR excesses around nearby late-M dwarfs using WISE data. Based on our SEDs and WISE images, we detected IR excess only in one target. The detection of IR excess in the source implies the presence of a disk around the target. In a forthcoming paper, we will present our further study of the target to confirm the nature of the disk.

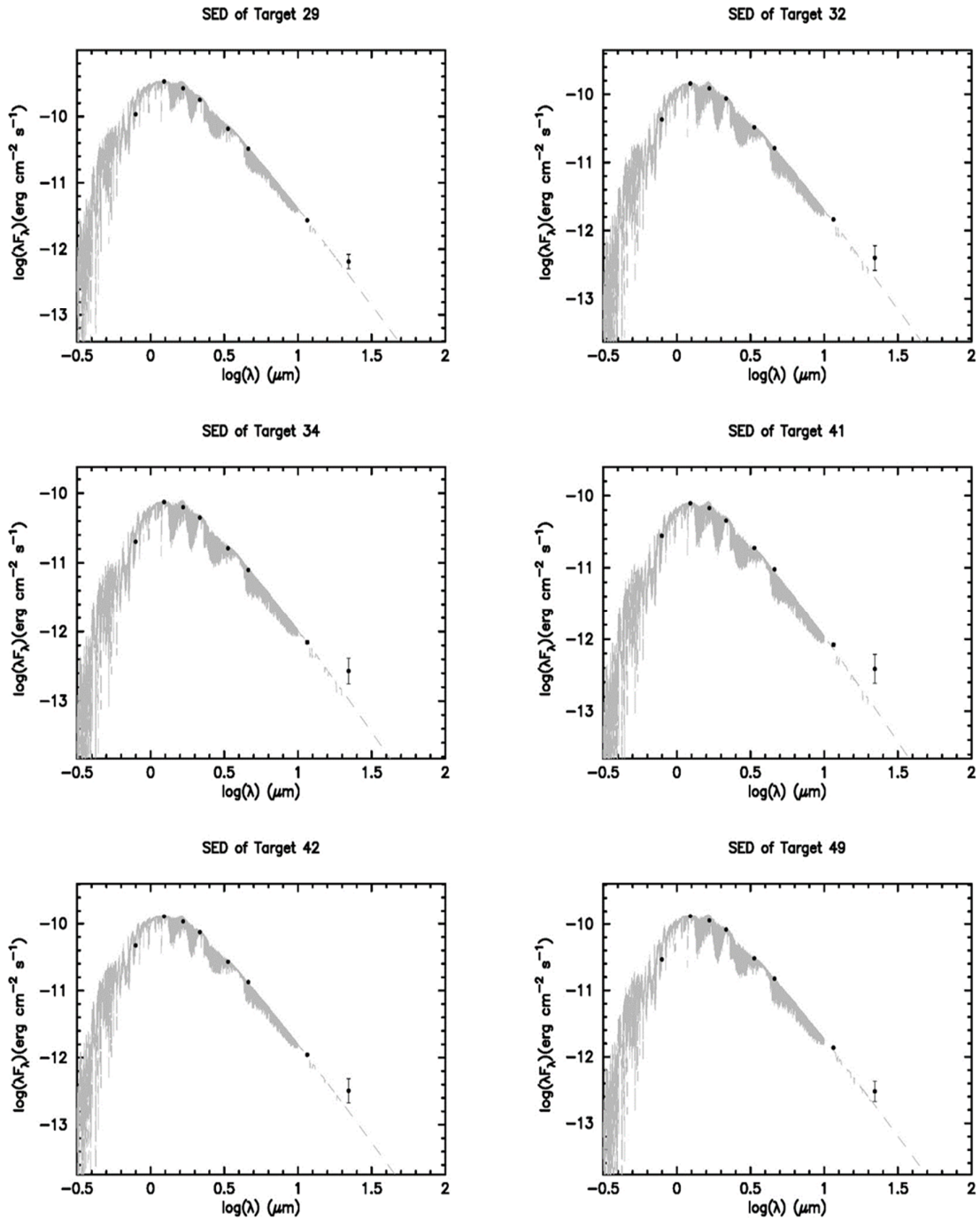


**Figure 1.** SEDs of 6 late-M dwarfs with the IR excess marginally detected at  $22 \mu\text{m}$ . The grey curve represents the best-fit model to the observed data points from DENIS, 2MASS and WISE (solid circles).

## SED of Target 58

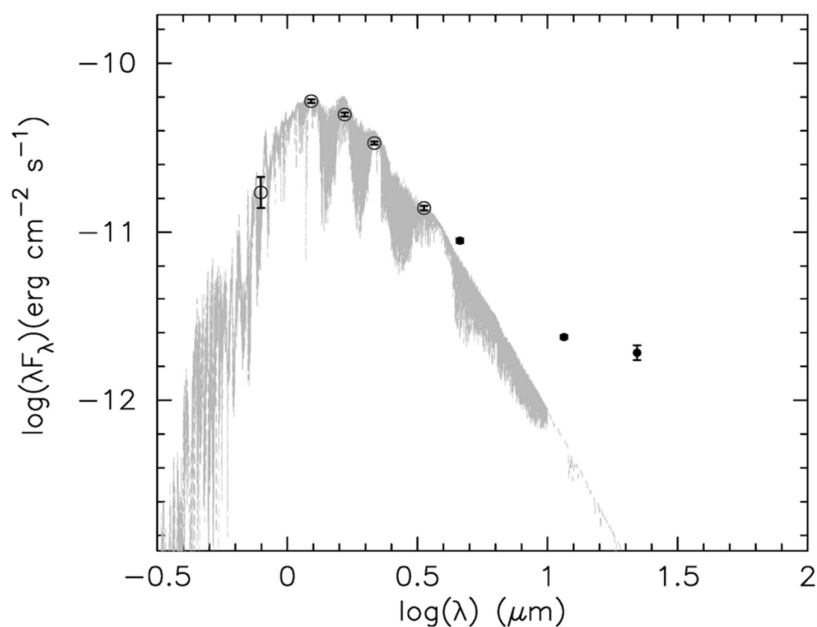


Figure 2. SED of target 58. The IR excesses are detected at 4.6  $\mu\text{m}$ , 12  $\mu\text{m}$  and 22  $\mu\text{m}$  (solid circles)

❖ **Conflict of Interest:** Authors have no conflict of interest to declare.

❖ **Acknowledgment:** This research is funded by Vietnam National Foundation for Science and Technology Development (NAFOSTED) under grant number 103.99-2015.108. This work makes use of the data products from the Wide-field Infrared Survey Explorer, which is a joint project of the University of California, Los Angeles, and the Jet Propulsion Laboratory (JPL)/Caltech, funded by NASA. This research also made use of the SIMBAD database and VizieR catalog access tool, operated at CDS, Strasbourg, France.

## REFERENCES

- [1] M. C. Wyatt, "Evolution of Debris Disks," *Annual Review of Astronomy and Astrophysics*, 46, 1, pp. 339-383, 2008.
- [2] J. P. Williams and L. A. Cieza, "Protoplanetary Disks and Their Evolution," *Annual Review of Astronomy and Astrophysics*, 49, 1, pp. 67-117, 2011.
- [3] A. P. Boss, "Rapid Formation of Super-Earths around M Dwarf Stars," *The Astrophysical Journal*, 644, 1, pp. L79-L82, 2006.
- [4] P. S. Muirhead, J. A. Johnson, A. Kevin, et al., "Characterizing the Cool KOIs. III. KOI 961: A Small Star with Large Proper Motion and Three Small Planets," *The Astrophysical Journal*, 747, 144, 16 pp, 2012.



- [5] M. Gillon, E. Jehin, S. M. Lederer, J. de Wit, et al., “Temperate Earth-sized planets transiting a nearby ultracool dwarf star,” *Nature*, 533, 7602, pp. 221-224, 2016.
- [6] M. Gillon, A. H. M. J. Triaud, B. Demory, et al., “Seven temperate terrestrial planets around the nearby ultracool dwarf star TRAPPIST-1,” *Nature*, 542, 7642, pp. 456-460, 2017.
- [7] H. Avenhaus, H. M. Schmid and M. R. Meyer, “The nearby population of M-dwarfs with WISE: a search for warm circumstellar dust,” *Astronomy and Astrophysics*, 548, A105, 15 pp, 2012.
- [8] A. S. Binks and R. D. Jeffries, “A WISE-based search for debris discs amongst M dwarfs in nearby, young, moving groups,” *Monthly Notices of the Royal Astronomical Society*, 469, 1, pp. 579-593, 2017.
- [9] C. A. Theissen and A. A. West, “Warm dust around cool stars: field M dwarfs with WISE 12 or 22  $\mu\text{m}$  excess emission,” *The Astrophysical Journal*, 794, 146, 28 pp, 2014.
- [10] J. F. Lestrade, M. C. Wyatt, F. Bertoldi, W. R. F. Dent, K. M. Menten, “Search for Cold Debris Disks around M-Dwarfs,” *Astronomy and Astrophysics*, 460, 3, pp. 733-741, 2006.
- [11] J. F. Lestrade, B. C. Matthews, B. Sibthorpe, “A Debris Disk around The Planet Hosting M-Star GJ 581 Spatially Resolved With Herschel,” *Astronomy and Astrophysics*, 548, A86, 15pp, 2012.
- [12] M. C. Liu, B. C. Matthews, J. P. Williams, P. G. Kalas, “A Submillimeter Search of Nearby Young Stars for Cold Dust: Discovery of Debris Disks around Two Low-Mass Stars,” *The Astrophysical Journal*, 608, 1, pp. 526-532, 2004.
- [13] A. Boucher, D. Lafrenière, et al, “BANYAN. VIII. New Low-mass Stars and Brown Dwarfs with Candidate Circumstellar Disks,” *The Astrophysical Journal*, 832, 50, 11 pp, 2016. (13)
- [14] S. J. Murphy, E. E. Mamajek, C. P. M. Bell, “WISE J080822.18-644357.3 - a 45 Myr-old accreting M dwarf hosting a primordial disc,” *Monthly Notices of the Royal Astronomical Society*, 476, 3, pp. 3290-3302, 2018.
- [15] F. Crifo, Ngoc Phan-Bao, X. Delfosse, et al., “New neighbours – VI. Spectroscopy of DENIS nearby stars candidates,” *Astronomy and Astrophysics*, 441, 2, pp. 653-661, 2005.
- [16] Ngoc Phan-Bao, J. Guifert, F. Crifo, et al., “New neighbours: IV. 30 DENIS late-M dwarfs between 15 and 30 parsecs,” *Astronomy and Astrophysics*, 380, pp. 590-598, 2001.
- [17] Ngoc Phan-Bao, F. Crifo, X. Delfosse, et al., “New neighbours: V. 35 DENIS late-M dwarfs between 10 and 30 parsecs,” *Astronomy and Astrophysics*, 401, pp. 959-974, 2003.
- [18] Ngoc Phan-Bao, E. L. Martín, C. Reylé, T. Forveille, J. Lim, “Discovery of a widely separated binary system of very low mass stars,” *Astronomy and Astrophysics*, 439, 2, pp. L19-L22, 2005.
- [19] Ngoc Phan-Bao, M.S. Bessell, “Spectroscopic Distance of Nearby Ultracool Dwarfs,” *Astronomy and Astrophysics*, 446, 2, pp. 515-523, 2006.
- [20] Ngoc Phan-Bao, M. S. Bessell, Dat Nguyen-Thanh, E. L. Martín, P.T.P. Ho, C. F. Lee, H. Parsons, “Detection of lithium in nearby young late-M dwarfs,” *Astronomy and Astrophysics*, 600, A19, 9 pp, 2017.
- [21] I. N. Reid, K. L. Cruz, et al., “Meeting the Cool Neighbors. VII. Spectroscopy of Faint Red NLTT Dwarfs,” *The Astronomical Journal*, 126, 6, pp. 3007-3016, 2003.

- [22] I. N. Reid, J. E. Gizis, "Probing the LHS Catalog. II. Faint Proper-Motion Stars," *The Publications of the Astronomical Society of the Pacific*, 117, 833, pp. 676-698, 2005.
- [23] K. L. Cruz, I. N. Reid, et al., "Meeting the Cool Neighbors. V. A 2MASS-Selected Sample of Ultracool Dwarfs," *The Astronomical Journal*, 126, 5, pp. 2421-2448, 2003.
- [24] G. Chabrier and I. Baraffe, "Theory of Low-Mass Stars and Substellar Objects," *Annual Review of Astronomy and Astrophysics*, 38, pp. 337-377, 2000.
- [25] G. Basri, "Observations of Brown Dwarfs," *Annual Review of Astronomy and Astrophysics*, 38, pp. 485-519, 2000.
- [26] M. Cohen, W.A. Wheaton, and S.T. Megeath, "Spectral Irradiance Calibration in the Infrared. XIV. The Absolute Calibration of 2MASS," *The Astronomical Journal*, 126, 2, pp. 1090-1096, 2003.
- [27] P. Fouqué, L. Chevallier, M. Cohen, et al., "An absolute calibration of DENIS (deep near infrared southern sky survey)," *Astronomy and Astrophysics Supplement*, 141, pp. 313-317, 2000.
- [28] T. H. Jarret, M. Cohen, F. Masci, et al., "The Spitzer-WISE Survey of the Ecliptic Poles," *The Astrophysical Journal*, 735, 112, 33 pp, 2011.
- [29] F. Allard, P. H. Hauschildt, I. Baraffe, G. Chabrier, "Synthetic Spectra and Mass Determination of the Brown Dwarf GI 229B," *Astrophysical Journal Letters*, 465, pp. L123-L127, 1996.